European Journal of Radiology 138 (2021) 109650

Contents lists available at ScienceDirect

European Journal of Radiology

journal homepage: www.elsevier.com/locate/ejrad

Research article

Correlation between lung ultrasound and chest CT patterns with estimation of pulmonary burden in COVID-19 patients

Francesco Rizzetto [a,*], Noemi Perillo [a], Diana Artioli [a], Francesca Travaglini [a], Alessandra Cuccia [a], Stefania Zannoni [a], Valeria Tombini [b], Sandro Luigi Di Domenico [b], Valentina Albertini [c], Marta Bergamaschi [b], Michela Cazzaniga [b], Cristina De Mattia [d], Alberto Torresin [d,e], Angelo Vanzulli [a,f], on behalf of the Niguarda COVID-19 Working Group

[a] Department of Radiology, ASST Grande Ospedale Metropolitano Niguarda, Piazza Ospedale Maggiore 3, 20162, Milan, Italy
[b] Emergency Department, ASST Grande Ospedale Metropolitano Niguarda, Piazza Ospedale Maggiore 3, 20162, Milan, Italy
[c] Postgraduate School of Emergency Medicine and Critical Care, Università degli Studi di Milano-Bicocca, Piazza dell'Ateneo Nuovo 1, 20126, Milan, Italy
[d] Department of Medical Physics, ASST Grande Ospedale Metropolitano Niguarda, Piazza Ospedale Maggiore 3, 20162, Milan, Italy
[e] Department of Physics, Università degli Studi di Milano, via Giovanni Celoria 16, 20133, Milan, Italy
[f] Department of Oncology and Hemato-Oncology, Università degli Studi di Milano, via Festa del Perdono 7, 20122, Milan, Italy

ARTICLE INFO

Keywords:
COVID-19
Lung
Ultrasonography
Tomography
X-Ray computed
Diagnostic techniques and procedures

ABSTRACT

Purpose: The capability of lung ultrasound (LUS) to distinguish the different pulmonary patterns of COVID-19 and quantify the disease burden compared to chest CT is still unclear.

Methods: PCR-confirmed COVID-19 patients who underwent both LUS and chest CT at the Emergency Department were retrospectively analysed. In both modalities, twelve peripheral lung zones were identified and given a Severity Score basing on main lesion pattern. On CT scans the well-aerated lung volume (%WALV) was visually estimated. *Per-patient* and *per-zone* assessments of LUS classification performance taking CT findings as reference were performed, further revisioning the images in case of discordant results. Correlations between number of disease-positive lung zones, Severity Score and %WALV on both LUS and CT were assessed. The area under receiver operating characteristic curve (AUC) was calculated to determine LUS performance in detecting % WALV $\leq$ 70 %.

Results: The study included 219 COVID-19 patients with abnormal chest CT. LUS correctly identified as positive 217 (99 %) patients, but *per-zone* analysis showed sensitivity = 75 % and specificity = 66 %. The revision of the 121 (55 %) cases with positive LUS and negative CT revealed COVID-compatible lesions in 42 (38 %) CT scans. Number of disease-positive zones, Severity Score and %WALV between LUS and CT showed moderate correlations. The AUCs for LUS Severity Score and number of LUS-positive zones did not differ in detecting % WALV $\leq$ 70 %.

Conclusion: LUS in COVID-19 is valuable for case identification but shows only moderate correlation with CT findings as for lesion patterns and severity quantification. The number of disease-positive lung zones in LUS alone was sufficient to discriminate relevant disease burden.

1. Introduction

Coronavirus Disease 2019 (COVID-19), caused by the Severe Acute Respiratory Syndrome Coronavirus 2 (SARS-CoV-2), was firstly reported in the Chinese province of Wuhan and then rapidly spread worldwide, being declared a pandemic on March 11, 2020 [1,2]. Since the beginning of the COVID-19 outbreak, many diagnostic approaches were attempted to early and reliably identify patients suspected of infection and to stratify them according to disease severity.

In this context, chest CT scan played a central role because of its high

Abbreviations: COVID-19, Coronavirus Disease 2019; IQR, interquartile range; LUS, lung ultrasound; NLR, negative likelihood ratio; PLR, positive likelihood ratio; SARS-CoV-2, Severe Acute Respiratory Syndrome Coronavirus 2; SE, sensitivity; SP, specificity; %WALV, well-aerated lung percentage.

* Corresponding author.
E-mail address: francesco.rizzetto@unimi.it (F. Rizzetto).

https://doi.org/10.1016/j.ejrad.2021.109650
Received 5 December 2020; Received in revised form 21 February 2021; Accepted 9 March 2021
Available online 11 March 2021

sensitivity (91–96 %) [3]. Typical, although non-specific, CT findings of COVID-19 include ground-glass opacities, crazy-paving patterns and areas of consolidation [4,5]. These alterations in COVID-19 are usually multiple, bilateral, patchy, segmental or sub-segmental, and mostly distributed along the bronchovascular bundles and the subpleural space [6,7]. With the progression of the disease, the lesions tend to increase and merge giving extensive lung involvement, up to provoke Acute Respiratory Distress Syndrome [8].

The typically peripheral distribution of COVID-19 makes lung ultrasound (LUS) particularly suitable to investigate this disease. Contrary to CT scan, which has high sensitivity but also limitations related to scanner availability, disinfection procedures and X-rays exposure, LUS is a quick, non-invasive, radiation risk-free and portable technique that can be obtained at the patient's bedside [9]. Consequently, it gained an increasing role in the early diagnosis and monitoring of patients with suspected or ascertained SARS-CoV-2 infection. The LUS of COVID-19 patients shows the same signs described in other lung diseases, such as B-lines and consolidations, but peculiar findings, like the "light beam" artifact, have also been described [10,11]. However, the attenuation of sound waves by the aerated pulmonary parenchyma hinders the possibility to study the central aspect of the lung, limiting the assessment to the peripheral zones [12,13]. Therefore, the actual capability of LUS to quantify lung involvement and disease severity and to stratify patients accordingly is still unclear.

The purpose of this study was to determine the correlation between LUS and CT findings in SARS-CoV-2 infection, to assess the performance of LUS to classify lung abnormalities and to evaluate the possibility of using this technique to provide a quantitative assessment of pulmonary involvement in COVID-19 patients.

2. Materials and methods

2.1. Patients

This study was retrospectively conducted in a single high-volume referral hospital for the management of the COVID-19 outbreak. The study was approved by the Local Ethics Committee (decision number: 188-22042020). Since data were collected retrospectively and processed anonymously, informed consent was waived.

Patients with COVID-19 who underwent both chest CT imaging and LUS within 24 h on admission to the Emergency Department from March 3, 2020 to April 4, 2020 were consecutively enrolled. Considering the high community prevalence of the disease in the period of enrolment [14] and the high specificity of nuclear acid amplification test [15], SARS-CoV-2 infection was confirmed through reverse-transcriptase polymerase chain reaction in at least one nasopharyngeal swab performed on admission or during hospitalisation.

2.2. Chest CT scanning protocol

Chest CT was performed with a dedicated 128-channel multidetector scan (Somatom Definition Edge VB10, Siemens Healthineers, Germany) with patients in supine position, during a single breath-hold, in keeping with the patient compliance. The main scanning parameters were: tube voltage = 100−120 kV (automatic kV setting, on basis of patient size – "Care kV"); automatic tube current modulation; pitch = 1; matrix = 512 × 512; collimation = 0.6 mm.

All images were reconstructed with slice thickness = 3 mm using a pulmonary BI57 kernel and a mediastinal Br38 kernel.

After every examination, the CT equipment and all positioning accessories were disinfected using damp cloths impregnated with a 75 % ethanol solution, according to the manufacturer recommendation. Three-time per day major disinfection of the surfaces of the whole CT room was also performed, including cleaning the floor with 2000 mg/L chlorine. Besides, an air disinfector was used for continuous disinfection of the equipment room.

2.3. CT image analysis

CT scans were analysed by three radiologists with 15, 14 and 9 years of experience in thoracic radiology, blinded to the clinical and LUS data. Three regions for each lung were considered: upper region (from apex to aortic arch), middle region (from aortic arch to right middle bronchus) and lower region (from right middle bronchus to the diaphragm). For each region, a peripheral area (outer one-third of lung) and a central area (inner two-third of lung) were distinguished on the axial slices, as previously suggested [16]. The peripheral areas were also divided into two zones (anterior and posterior) based on a coronal plane passing through the tracheal carina. Each of the 12 peripheral zones thus identified was assigned a Severity Score from 0 to 3 based on the prevalent lesion patterns as defined by the Fleischner Society Glossary [17,18]: normal = 0; ground-glass opacity = 1; crazy-paving = 2; consolidation = 3 (Fig. 1).

The scores of the single zones were summed and the resulting total CT Severity Score was reported. A zone with a score >0 was defined as a CT-positive zone.

The radiologists also performed a visual estimation of the well-aerated lung volume expressed as percentage (%WALV) of the total lung volume, rounded to the nearest 10 %.

Each radiologist evaluated approximately one-third of the total patients; moreover, in a randomly chosen subset of 54 patients, the CT Severity Score and the %WALV were independently assessed by all three radiologists to evaluate inter-reader reproducibility.

2.4. Lung ultrasound protocol

A wheeled ultrasound machine (MyLab™Alpha, Esaote Italia, Genova, Italy) dedicated only to patients suspected of having COVID-19 infection was used. The machine was prepared using a single plastic cover for the probe and cleaning the tablet with a 75 % ethanol solution. Convex probes (3.5 MHz) and single focal point modality set on the pleura line were used to allow a quick overall evaluation of the entire chest and provide more depth penetration [19].

The patients were examined preferably in a seated position, or supine when sitting was impossible, having the care to rotate them to evaluate the posterior fields.

Scans orthogonal to the ribs were firstly used to find the best location; then, the probe was turned to perform intercostal scans, in order to cover the widest surface.

2.5. Lung Ultrasound image analysis

LUS was performed at admission in the Emergency Department by 31 experienced clinicians.

Three regions (upper, middle and lower) of the lung were considered, each one divided in an anterior and a posterior zone, on both sides. The protocol to divide the lung zones was similar to that used in the emergency setting to investigate the entire chest surface with a limited number of scans [20,21]. For the anterior region, the upper zone was acquired on the midclavicular line above the inter-nipple line, the middle zone on the anterior axillary line below the inter-nipple line, and the inferior zone on the medium axillary line. The zones of the dorsal region were divided using as reference the scapular spine and the inferior scapular angle.

The resulting 12 zones were scored considering the number and morphology of B-lines [22,23] as follows: normal A lines = 0; separated B-lines = 1; coalescent B-lines = 2; consolidation = 3 (Fig. 2), as reported by Volpicelli et al. [10].

The total LUS Severity Score resulting from the sum of single-zone scores was reported.

A zone with a score >0 was defined as a LUS-positive zone.

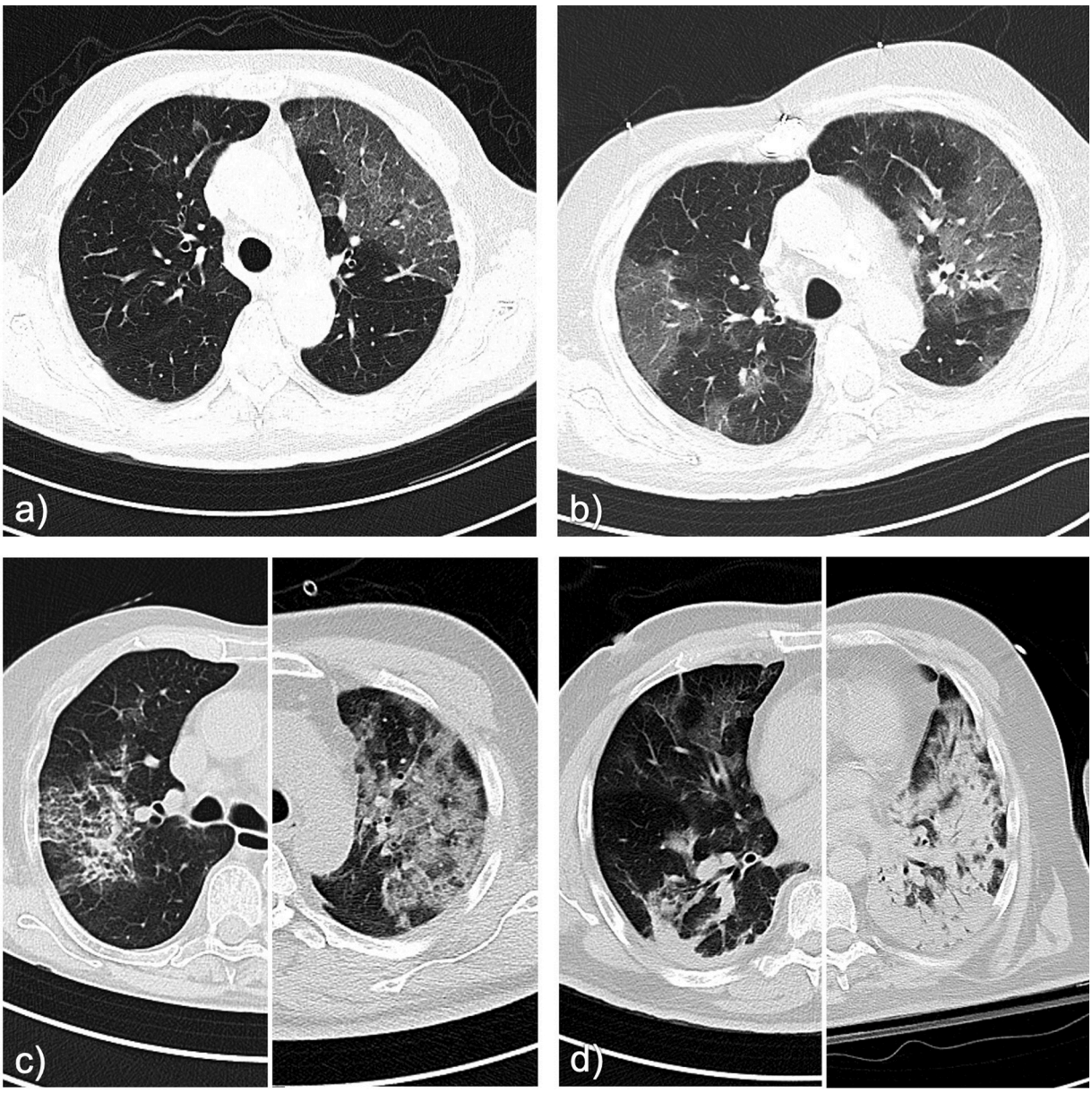

Fig. 1. Examples of CT patterns: *a*) normal pulmonary parenchyma (Severity Score = 0) in the anterior and posterior zones of the right lung, while GGOs (Severity Score = 1) are visible in the anterior zone of the left lung; *b*) bilateral diffuse GGOs (Severity Score = 1); *c*) two examples of crazy paving pattern (Severity Score = 2), with predominant septal thickening on the left panel and in progression to consolidation on the right panel; *d*) two examples of consolidations (Severity Score = 3), localized to the posterior lung zone on the left panel and widely distributed on the right panel.

2.6. Assessment of the CT-LUS disagreements

In case of disagreement between CT and LUS, i.e. when a lung zone had a LUS Severity Score > 0 and a CT Severity Score = 0, one of the radiologists carefully performed an unblinded revision of the CT imaging to assess the reason for disagreement. Findings were classified as follows: confirmed LUS false positive (i.e. no lesions detectable in CT); non-COVID-19 lesions (e.g. interstitial fibrosis, emphysema, nodules, etc.); COVID-compatible lesions; and topographic misinterpretation (i.e. presence of lesions at the border between two zones whose location assignment may have been ambiguous).

2.7. Statistical analysis

Categorical variables were expressed as counts and percentage, while median and interquartile range (IQR) were reported for discrete and continuous variables.

LUS ability to identify COVID-19 patients with lung alterations was evaluated by considering the number of patients classified as positive (at least one positive lung zone) or negative (no positive lung zones) by both LUS and CT scan.

Sensitivity (SE) and specificity (SP) of LUS for the different lung zones of each patient were assessed taking chest CT findings as a reference since the latter is considered the standard for studying pulmonary lesions. Chi-square test was used to assess the null hypothesis that there were no differences between different lung zones in terms of LUS SE and SP and CT Severity Score.

After the revision of the cases of disagreement between CT and LUS, SE and SP were recalculated, considering as LUS false positive results only the zones without lung abnormalities or with non-COVID-19 lesions in the CT imaging.

The inter-reader agreement for both the CT Severity Score and %

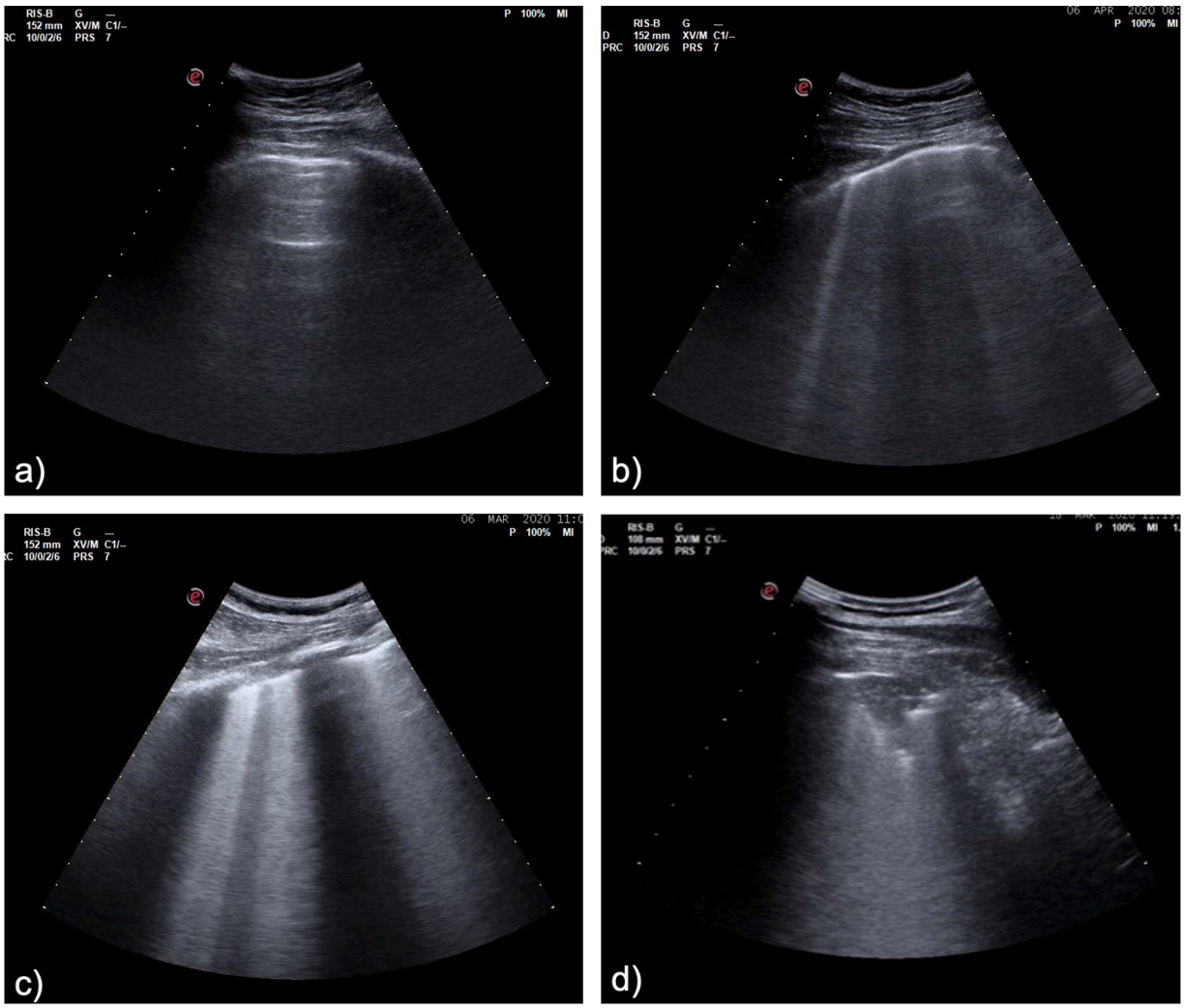

Fig. 2. Example of lung ultrasound patterns in COVID-19: *a*) lines A (Severity Score = 0); *b*) separated lines B (Severity Score = 1); *c*) coalescent lines B (Severity Score = 2); *d*) consolidations (Severity Score = 3).

WALV was tested using the intra-class correlation coefficient (ICC) based on a single rater 2-way random-effects model, following Koo et al. for its interpretation [24].

Spearman's *rho* correlation coefficient was used to evaluate the correlation between: number of CT-positive zones and LUS-positive zones; CT Severity Score and LUS-Severity Score; %WALV and number of LUS-positive zones; %WALV and LUS Severity Score. A *rho* coefficient >0.7 was considered strong [25].

Receiver operating characteristic (ROC) curve analysis was calculated to assess the performance of the number of LUS-positive zones and LUS Severity Score to help differentiate patients with %WALV above or below 70 %. This %WALV was chosen since previously reported as correlated with severe outcome in COVID-19 patients [16,26].

The areas under the ROC curves (AUCs) were calculated and compared with Delong method [27]. For each number of LUS-positive zones and each LUS Severity Score, SE, SP, positive likelihood ratio (PLR) and negative likelihood ratio (NLR) for identifying patients with %WALV $\leq$ 70 % were calculated. The cut-offs providing NLR < 0.1 (discard point) and PLR > 10 (confirmation point) were selected [28].

Statistical significance was established at the $p < 0.05$ level, applying Bonferroni's correction for multiple comparisons when appropriate. Considering $\alpha = 0.05$ and at least a low correlation (*rho*>0.30) between CT and LUS findings, a sample size of 195 patients provides a study power = 99 %.

The data analysis was generated using the Real Statistics Resource Pack software (Release 6.8) (www.real-statistics.com) and R software (v.3.5.1).

3. Results

A total of 238 patients were initially enrolled, of whom 11 were excluded because of artifacts in the chest CT and 8 were excluded because the LUS Severity Score was not recorded. The 219 patients finally included were 152 (69 %) males and 67 (31 %) females and had a median age of 58 years (IQR: 49–71 years) and a median Body Mass Index of 26 kg/m^2 (IQR: 24–29 kg/m^2), with 46 (21 %) obese patients (Body Mass Index >30 kg/m^2). Pre-existing pathologies, including cardiovascular diseases, active neoplastic disease and chronic kidney disease, were reported for 145 (66 %) patients. The median time between the onset of patients' symptoms and the execution of imaging procedures was 7 days (IQR: 5–10 days). Demographic data are reported in Table 1.

All 219 (100 %) patients had visible pulmonary involvement at the chest CT. Lesions in at least one central lung area without involvement of the corresponding periphery were observed in 26 (12 %) patients, while only 2 (1%) patients had exclusively central involvement.

The median number of CT-positive zones was 9 (IQR: 6–11), the median CT Severity Score was 13 (IQR: 9–18) and the median %WALV was 60 % (IQR: 40–80 %). Posterior zones of middle and lower lung regions showed higher CT Severity Score than the corresponding

Table 1
Clinical data of patients at admission in the Emergency Department. Median and interquartile range are reported for continuous variables.

Variables	All patients (n = 219)
Age (years)	58 (49–71)
Gender	
Male	152 (69 %)
Female	67 (31 %)
Smoking history	
Unknown	79 (36 %)
Never	122 (54 %)
Former	9 (4%)
Current	9 (4%)
Body Mass Index (kg/m^2)	26 (24–29)
Body Mass Index >30 kg/m^2 (obesity)	46 (21 %)
Comorbidities	145 (66 %)
Cardiovascular disease	29 (13 %)
Pulmonary disease	5 (2%)
Oncological disease	9 (4%)
Hypertension	91 (42 %)
Diabetes	32 (15 %)
Chronic kidney disease	12 (5%)
Other	61 (28 %)
Time between symptoms onset and imaging (days)	7 (5–10)

anterior zones ($p < 0.001$). The *per zone* distribution of the assigned CT scores was illustrated in Fig. 3. Inter-reader agreement for both CT Severity Score and %WALV was good to excellent, with an ICC of 0.84 (95 %CI: 0.75–0.90) and 0.93 (95 %CI: 0.90–0.96), respectively.

The median number of LUS-positive zones was 8 (IQR: 5–10) and the median LUS Severity Score was 12 (IQR: 6–17).

The LUS failed to detect lung involvements in only 2 (1%) patients, while it correctly classified all the other patients. However, when assessing the different lung zones independently, the overall SE and SP of LUS taking the CT findings as reference were 75 % (1348/1801; 95 % CI: 73–77 %) and 66 % (549/827; 95 %CI: 63–70 %), respectively. Comparing SE and SP for each zone (Fig. 4), a significantly better LUS SE was found for the posterior zones of the medium and lower lung regions bilaterally. In particular, SE in these posterior zones ranged between 87 % and 88 % while it ranged between 66 % and 69 % in the corresponding anterior ones. A lower SE was observed for the left upper zones (62 % anteriorly and 64 % posteriorly), although only slightly below the corrected *p*-value cut-off. SP between different zones varied from 53 % to 78 %, but differences were not statistically significant.

A total of 121 (55 %) patients had at least a lung zone with a LUS Severity Score >0 and a CT Severity Score = 0. The second unblinded reading of these zones revealed that there were no abnormalities of the pulmonary parenchyma (i.e. confirmed LUS false positive) in only 8 (6%) cases. For the rest of these patients, 71 (59 %) showed lung abnormalities, 42 (38 %) of which COVID-compatible, mainly represented by micro-areas of ground-glass opacity or very faint low-contrast lesions (Fig. 5). In the remaining 42 (35 %) out of 121 patients, the disagreement between CT and LUS was related to lesions at the border between two zones, which likely led to a not-corresponding location assignment of the disease findings.

Based on the result of this revision, the overall SE and SP recalculated on all lung zones were 77 % (1539/1991; 95 %CI: 75–79 %) and 86 % (550/637: 95 %CI: 83–89 %), respectively.

Only a moderate positive correlation was found between the numbers of CT- and LUS-positive zones ($rho = 0.59$, $p < 0.001$) and between the CT and LUS Severity Score ($rho = 0.60$, $p < 0.001$) (Fig. 6a and b). Considering the %WALV, a moderate negative correlation with both the number of LUS-positive zones (rho=–0.67, $p < 0.001$) and LUS Severity Score (rho=–0.69, $p < 0.001$) was found (Fig. 6c and d).

The diagnostic performance of LUS in identifying COVID-19 patients with a %WAL ≤ 70 % was reported in Fig. 7, considering both the LUS Severity Score and the number of LUS-positive zones. The AUCs for the two evaluations were of 0.87 (95 %CI: 0.81–0.93) and 0.86 (95 %CI: 0.80–0.92), respectively. These values were not significantly different ($p = 0.882$).

The sensitivity and specificity for each consecutive cut-off point, including the corresponding PLR and NLR, were reported in Table 2. For the LUS Severity Score a discard point of 4 (SE: 97 %; SP: 37 %; NLR: 0.09) and a confirmation point of 17 (SE: 40 %; SP: 97 %; PLR: 13.51) were found. For the number of LUS-positive zones, the discard point was 3 (SE: 97 %; SP: 35 %; NLR: 0.09) and the confirmation point was 11 (SE: 34 %; SP: 99 %; PLR: 22.97).

4. Discussion

The overwhelming burden placed on health systems by the COVID-19 pandemic prompted the use of LUS since more rapid and manageable to assess patients suspected of infection than chest CT. In the current study, almost all patients with lung abnormalities on the chest CT scan were correctly classified as positive by LUS, showing its reliability for case identification. This corresponds with the current results of the literature, which reports a very high sensitivity (89–100 %) for the diagnosis of COVID-19 [29–31].

The fact that central lung involvement without peripheral lesions was only rarely found further supports the role of LUS in the evaluation of COVID-19 patients. With the progression of the SARS-CoV-2 infection, the quantity of air in the involved pulmonary parenchyma decreases and the lesions tend to spread and become confluent [32]. Accordingly, the higher sensitivity of LUS observed for the posterior zones could be explained by the greater severity of the lesions in these sites that are usually first and peripherally involved by the disease [33,34].

Moreover, the revision of the zonal disagreements between CT and LUS revealed that in almost all cases there were underlying abnormalities. Regarding the COVID-compatible lesions initially missed on CT, they were very small or low-contrast areas of parenchymal opacification, easy to be overlooked or to be misinterpreted as motion artifacts or dystelectasis. These findings seemed to corroborate the hypothesis that LUS is able to reveal COVID-19 lesions even in a very early stage thanks to its tissue resolution superior to CT scan [35]. However, these results should be interpreted with caution, since the lesions identified were compatible with COVID-19 but they were not specific [36] and no follow-up imaging was available to confirm their nature. Also, it must be

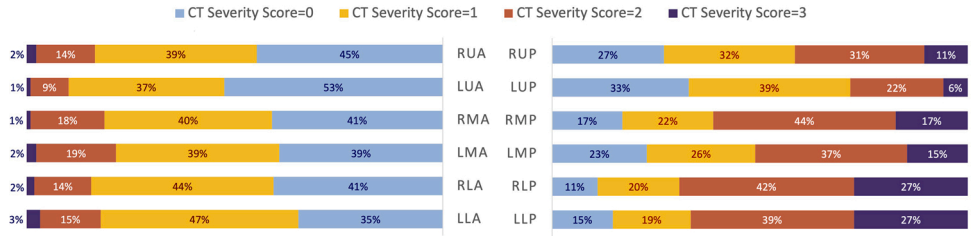

Fig. 3. Distribution of the CT Severity Score values in the different zones of the lungs expressed as percentage of the total scores (n = 219) assigned to each zone. The lung zones were named after the following three-letter code: first letter: Right (R) or Left (L); second letter: Upper (U), Middle (M) or Lower (L); third letter: Anterior (A) or Posterior (P).

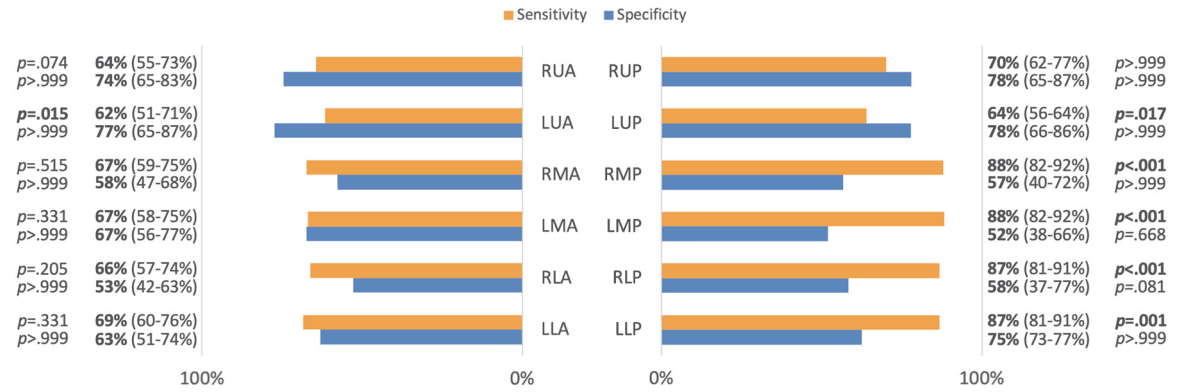

Fig. 4. Sensitivity and specificity (95 % confidence interval in parentheses) of lung ultrasound for each of the 12 peripheral zones identified in the lungs. CT findings were used as reference. The *p* values adjusted after Bonferroni's correction were reported, referring to the null hypothesis that there were no differences between different lung zones in terms of sensitivity and specificity. The lung zones were named after the following three-letter code: first letter: Right (R) or Left (L); second letter: Upper (U), Middle (M) or Lower (L); third letter: Anterior (A) or Posterior (P).

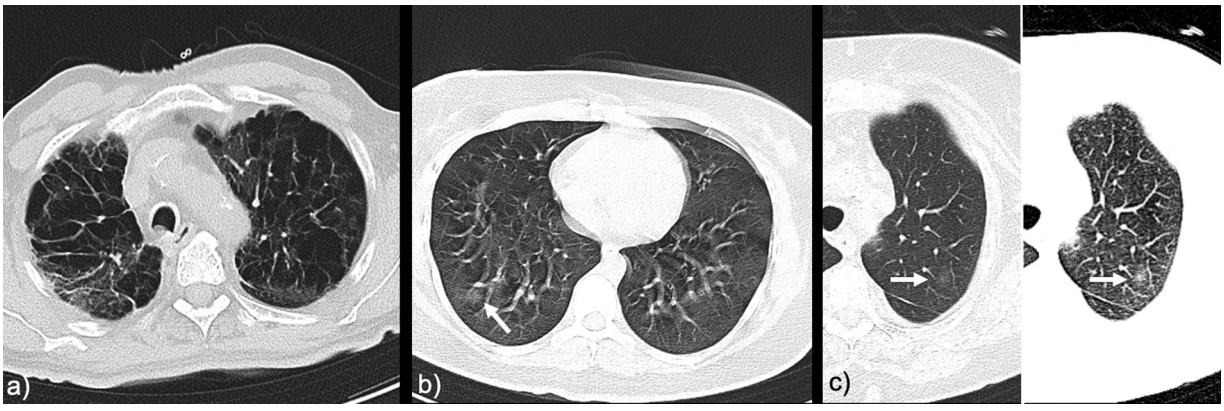

Fig. 5. Examples from different patients of reviewed lung zones with discordant findings between lung ultrasound (Severity Score>0) and chest CT (Severity Score = 0): *a*) bilateral emphysema and interstitial fibrosis of the upper lung zones (non-COVID-19 lesions); *b*) a small round COVID-compatible opacity (*arrow*) is visible in the lower posterior zone of the right lung, despite confusable with the motion artifacts; *c*) a very low-contrast COVID-compatible opacity (*arrows*) is present in the upper posterior zone of the left lung, barely visible in the routine preset lung window (left panel) but more evident narrowing the window (right panel).

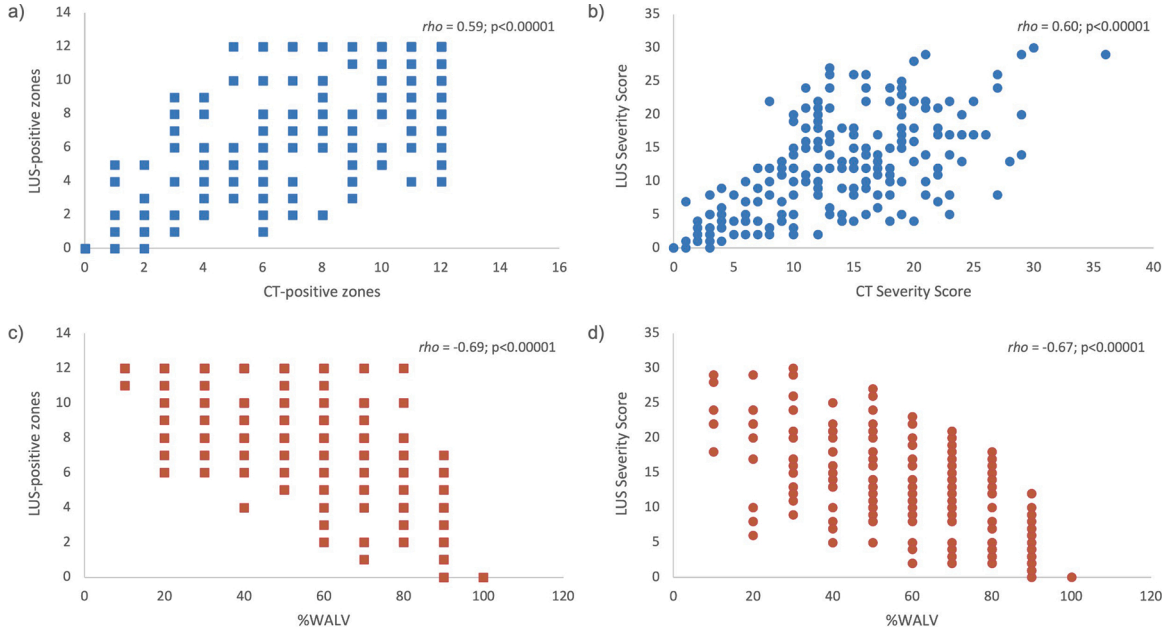

Fig. 6. Correlation between number of CT-positive zones and number of LUS-positive score (*a*), CT Severity Score and LUS Severity Score (*b*), percentage of well-aerated lung volume (%WALV) and LUS-positive zones (*c*) and %WALV and LUS Severity Score (*d*). Spearman's *rho* coefficient and *p* values are reported.

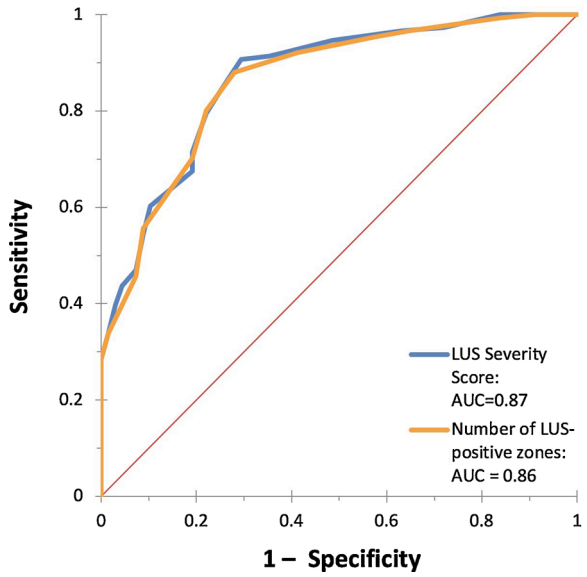

Fig. 7. Receiver Operator Curves of lung ultrasound (LUS) Severity Score and number of LUS-positive zones for detecting COVID-19 patients with % WALV ≤ 70 %.

underlined that the post-analysis revision could have been biased by the "reader expectation" [37], so that those findings that would have been otherwise classified as non-specific or even non-pathological were considered true lesions.

Additionally, LUS has to face the limited penetration of the ultrasound beam in the central pulmonary zones and the constraint of studying the lungs only through specific acoustic windows, which may leave unexplored regions. Actually, in the *per patient* analysis LUS performed very well since the detection of just one lung zone was sufficient to classify the COVID-19 patient as positive. On the contrary, the *per zone* performance was lower due to false positive and false negative findings that affected the LUS scoring system, which is congruent with previous works that demonstrated only a fair-to-moderate localization agreement between LUS and CT findings [31,38]. This may explain why CT and LUS severity indices appeared to be correlated but with a considerable dispersion of the values around the hypothetical trendline. For each number of CT-positive zones, a wide range of LUS-positive zones was found, so that for equal CT Severity Score the LUS Severity Score fluctuated, weakening the correlation between the two.

The same occurred with regard to the %WALV and, remarkably, no difference in performance was observed using the number of LUS-positive zones or the LUS Severity Score to discriminate patients with %WALV above or below 70 %. This finding is not surprising considering that the Severity Score is primarily dependent on the correct identification of the zones involved by the disease, but it is also consistent with the hypothesis that interstitial patterns and consolidations contribute similarly to the severity of lung impairment in COVID-19 patients [9].

Accordingly, the LUS cut-offs needed to confirm a relevant lung disease were very high (i.e. 11 LUS-positive zones or LUS Severity Score≥17), which may limit their application in clinical practice. On the contrary, a discard cut-off corresponding to LUS-positive zones ≤3 could be implemented to support the stratification of the patients and the detection of already advanced disease, even though other cut-offs with poorer NLR but better SP could even be considered (e.g., with 5 LUS-positive zones there would be 8% false positive cases but SP would rise from 35 % to 59 %).

The main limitation of this study is the possible existence of selection bias since only COVID-19-confirmed patients were retrospectively enrolled. Related to this, only *per zone* and not *per patient* SE and SP of LUS could be assessed. However, this study did not focus on the diagnostic performance but aimed to assess the correlation of LUS findings with ascertained COVID-19 lesions whose pattern was defined through CT imaging. Already in this setting, the misclassification of lung zones by LUS limited its ability to provide a reliable quantitative assessment of pulmonary involvement and, if patients without COVID-19 had been included, the impact would likely have been even greater.

Also, the analysed CT scans had a slice thickness of 3 mm, whereas the ideal thickness to study pulmonary interstitium is 1 mm; however, this was meant to improve the signal-to-noise ratio of low-contrast lesions and face the high-volume flow of patients to examine in the emergency setting. Another limitation was the number of CT and LUS readers involved in the study. According to the ICC, the reproducibility of the CT Severity Score and the visual estimation of the %WALV was high between the three radiologists, so that it can be assumed inter-reader variability did not affect the observed results. By contrast, the inter-reader agreement between LUS operators could not be estimated.

Table 2
Cut-off points of the LUS Severity Score and the number of LUS-positive zones with corresponding diagnostic indicators for identifying COVID-19 patients with a %WALV ≤ 70 %.

LUS Severity Score				
Cutoff	SE	SP	PLR	NLR
0	100 %	0%	1.00	–
1	100 %	9%	1.10	–
2	100 %	16 %	1.19	–
3	97 %	28 %	1.35	0.09
4	97 %	37 %	1.53	0.09
5	95 %	51 %	1.95	0.10
6	92%	62 %	2.41	0.13
7	91 %	65 %	2.59	0.13
8	91 %	71 %	3.08	0.13
9	84%	75 %	3.36	0.21
10	79 %	78 %	3.60	0.26
11	72 %	81 %	3.74	0.35
12	68%	81 %	3.53	0.40
13	60 %	90 %	5.85	0.44
14	54 %	91 %	6.15	0.50
15	47%	93 %	6.39	0.57
16	44%	96 %	9.91	0.59
17	40 %	97 %	13.51	0.62
18	34 %	99 %	22.97	0.67
19	28 %	100 %	–	0.72
20	26%	100 %	–	0.74
21	23%	100 %	–	0.77
22	19%	100 %	–	0.81
23	12 %	100 %	–	0.88
24	11%	100 %	–	0.89
25	7%	100 %	–	0.93
26	7%	100 %	–	0.93
27	4%	100 %	–	0.96
28	3%	100 %	–	0.97
29	3%	100 %	–	0.97
30	1%	100 %	–	0.99
Number of LUS-positive zones				
Cutoff	SE	SP	PLR	NLR
0	100 %	0%	1.00	–
1	100 %	9%	1.10	0.00
2	99 %	16 %	1.19	0.04
3	97 %	35 %	1.49	0.09
4	95 %	43 %	1.66	0.11
5	92%	59 %	2.24	0.14
6	88 %	72 %	3.15	0.17
7	80 %	78 %	3.63	0.25
8	70 %	81 %	3.67	0.37
9	56%	91 %	6.30	0.49
10	46%	93 %	6.21	0.59
11	34 %	99 %	22.97	0.67
12	28 %	100 %	–	0.72

LUS: lung ultrasounds; SE: Sensitivity; SP: Specificity; PLR: Positive Likelihood Ratio; NLR: Negtaive Likelihood Ratio.

However, since a high number of operators was involved it is reasonable to believe this provided a realistic picture of LUS performance in real-life clinical practice. A multicentre assessment of the influence of different LUS machines on the results is also mandatory.

Finally, the relationship between CT and LUS findings was investigated but no correlation with patients' outcomes was considered, which requires further studies to demonstrate the diagnostic and prognostic impact of the reported results.

In conclusion, LUS has a great *per patient* performance in identifying pulmonary alterations but, when moving to the *per zone* evaluation, it did not seem able to replicate the same quantitative information about lung involvement in COVID-19 provided by the CT imaging, especially in terms of lesion patterns. The number of LUS-positive zones alone can still be sufficient to discriminate patients with a relevant pulmonary burden and may facilitate their management and clinical stratification.

Funding

The authors state that this work has not received any funding.

CRediT authorship contribution statement

Francesco Rizzetto: Data curation, Formal analysis, Visualization, Writing - original draft, Writing - review & editing. **Noemi Perillo:** Data curation, Writing - original draft, Writing - review & editing. **Diana Artioli:** Investigation, Methodology, Writing - review & editing. **Francesca Travaglini:** Investigation, Methodology, Writing - review & editing. **Alessandra Cuccia:** Investigation, Methodology, Writing - review & editing. **Stefania Zannoni:** Investigation. **Valeria Tombini:** Investigation, Methodology, Writing - review & editing. **Sandro Luigi Di Domenico:** Investigation. **Valentina Albertini:** Investigation. **Marta Bergamaschi:** Investigation. **Michela Cazzaniga:** Investigation. **Cristina De Mattia:** Formal analysis, Validation, Writing - review & editing. **Alberto Torresin:** Formal analysis, Validation, Writing - review & editing. **Angelo Vanzulli:** Conceptualization, Supervision, Writing - review & editing.

Declaration of Competing Interest

The authors of this manuscript declare no relationships with any companies, whose products or services may be related to the subject matter of the article.

References

[1] World Health Organization, Novel Coronavirus (2019-nCoV) Situation Report - 11, Geneva (Switzerland), 2020, https://www.who.int/docs/default-source/coronaviruse/situation-reports/20200131-sitrep-11-ncov.pdf.
[2] World Health Organization, Coronavirus Disease 2019 (COVID-19) Situation Report – 51, Geneva (Switzerland), 2020, https://www.who.int/docs/default-source/coronaviruse/situation-reports/20200311-sitrep-51-covid-19.pdf.
[3] H. Kim, H. Hong, S.H. Yoon, Diagnostic performance of CT and reverse transcriptase-polymerase chain reaction for coronavirus disease 2019: a meta-analysis, Radiology (2020), 201343, https://doi.org/10.1148/radiol.2020201343.
[4] J.P. Kanne, B.P. Little, J.H. Chung, B.M. Elicker, L.H. Ketai, Essentials for radiologists on COVID-19: an update— radiology scientific expert panel, Radiology 78 (2020), 200527, https://doi.org/10.1148/radiol.2020200527.
[5] W. Yang, A. Sirajuddin, X. Zhang, G. Liu, Z. Teng, S. Zhao, M. Lu, The role of imaging in 2019 novel coronavirus pneumonia (COVID-19), Eur. Radiol. 30 (2020) 4874–4882, https://doi.org/10.1007/s00330-020-06827-4.
[6] F. Pan, T. Ye, P. Sun, S. Gui, B. Liang, L. Li, D. Zheng, J. Wang, R.L. Hesketh, L. Yang, C. Zheng, Time course of lung changes at chest CT during recovery from coronavirus disease 2019 (COVID-19), Radiology 295 (2020) 715–721, https://doi.org/10.1148/radiol.2020200370.
[7] J. Wu, J. Pan, D. Teng, X. Xu, J. Feng, Y.C. Chen, Interpretation of CT signs of 2019 novel coronavirus (COVID-19) pneumonia, Eur. Radiol. 30 (2020) 5455–5462, https://doi.org/10.1007/s00330-020-06915-5.
[8] F. Zhou, T. Yu, R. Du, G. Fan, Y. Liu, Z. Liu, J. Xiang, Y. Wang, B. Song, X. Gu, L. Guan, Y. Wei, H. Li, X. Wu, J. Xu, S. Tu, Y. Zhang, H. Chen, B. Cao, Clinical course and risk factors for mortality of adult inpatients with COVID-19 in Wuhan, China: a retrospective cohort study, Lancet 395 (2020) 1054–1062, https://doi.org/10.1016/S0140-6736(20)30566-3.
[9] G. Volpicelli, A. Lamorte, T. Villén, What's new in lung ultrasound during the COVID-19 pandemic, Intensive Care Med. 46 (2020) 1445–1448, https://doi.org/10.1007/s00134-020-06048-9.
[10] G. Volpicelli, L. Gargani, Sonographic signs and patterns of COVID-19 pneumonia, Ultrasound J. 12 (2020) 22, https://doi.org/10.1186/s13089-020-00171-w.
[11] S. Sofia, A. Boccatonda, M. Montanari, M. Spampinato, D. D'ardes, G. Cocco, E. Accogli, F. Cipollone, C. Schiavone, Thoracic ultrasound and SARS-COVID-19: a pictorial essay, J. Ultrasound 23 (2020) 217–221, https://doi.org/10.1007/s40477-020-00458-7.
[12] G. Lepri, M. Orlandi, C. Lazzeri, C. Bruni, M. Hughes, M. Bonizzoli, Y. Wang, A. Peris, M. Matucci-Cerinic, The emerging role of lung ultrasound in COVID-19 pneumonia, Eur. J. Rheumatol. 7 (2020) S129–S133, https://doi.org/10.5152/eurjrheum.2020.2063.
[13] M. Sperandeo, M.G. Tinti, G. Rea, Chest ultrasound versus chest X-rays for detecting pneumonia in children: Why compare them each other if together can improve the diagnosis? Eur. J. Radiol. 93 (2017) 291–292, https://doi.org/10.1016/j.ejrad.2017.05.038.
[14] A. Odone, D. Delmonte, T. Scognamiglio, C. Signorelli, COVID-19 deaths in Lombardy, Italy: data in context, Lancet Public Heal. 5 (2020) e310, https://doi.org/10.1016/S2468-2667(20)30099-2.
[15] B. Böger, M.M. Fachi, R.O. Vilhena, A.F. Cobre, F.S. Tonin, R. Pontarolo, Systematic review with meta-analysis of the accuracy of diagnostic tests for COVID-19, Am. J. Infect. Control 49 (2021) 21–29, https://doi.org/10.1016/j.ajic.2020.07.011.
[16] D. Colombi, F.C. Bodini, M. Petrini, G. Maffi, N. Morelli, G. Milanese, M. Silva, N. Sverzellati, E. Michieletti, Well-aerated Lung on Admitting Chest CT to Predict Adverse Outcome in COVID-19 Pneumonia, Radiology (2020), 201433, https://doi.org/10.1148/radiol.2020201433.
[17] D.M. Hansell, A.A. Bankier, H. MacMahon, T.C. McLoud, N.L. Müller, J. Remy, Fleischner society: glossary of terms for thoracic imaging, Radiology 246 (2008) 697–722, https://doi.org/10.1148/radiol.2462070712.
[18] A. Oikonomou, P. Prassopoulos, Mimics in chest disease: interstitial opacities, Insights Imaging 4 (2013) 9–27, https://doi.org/10.1007/s13244-012-0207-7.
[19] S.M. Efremov, V.V. Kuzkov, E.V. Fot, M.Y. Kirov, D.N. Ponomarev, R.E. Lakhin, E. A. Kokarev, Lung ultrasonography and cardiac surgery: a narrative review, J. Cardiothorac. Vasc. Anesth. 34 (2020) 3113–3124, https://doi.org/10.1053/j.jvca.2020.01.032.
[20] G. Soldati, A. Smargiassi, R. Inchingolo, D. Buonsenso, T. Perrone, D.F. Briganti, S. Perlini, E. Torri, A. Mariani, E.E. Mossolani, F. Tursi, F. Mento, L. Demi, Proposal for international standardization of the use of lung ultrasound for patients with COVID-19, J. Ultrasound Med. 39 (2020) 1413–1419, https://doi.org/10.1002/jum.15285.
[21] G. Volpicelli, M. Elbarbary, M. Blaivas, D.A. Lichtenstein, G. Mathis, A. W. Kirkpatrick, L. Melniker, L. Gargani, V.E. Noble, G. Via, A. Dean, J.W. Tsung, G. Soldati, R. Copetti, B. Bouhemad, A. Reissig, E. Agricola, J.J. Rouby, C. Arbelot, A. Liteplo, A. Sargsyan, F. Silva, R. Hoppmann, R. Breitkreutz, A. Seibel, L. Neri, E. Storti, T. Petrovic, International evidence-based recommendations for point-of-care lung ultrasound. Intensive Care Med, Springer, 2012, pp. 577–591, https://doi.org/10.1007/s00134-012-2513-4.
[22] S. Moore, E. Gardiner, Point of care and intensive care lung ultrasound: a reference guide for practitioners during COVID-19, Radiography 26 (2020) e297–302, https://doi.org/10.1016/j.radi.2020.04.005.
[23] B. Bouhemad, S. Mongodi, G. Via, I. Rouquette, Ultrasound for "lung monitoring" of ventilated patients, Anesthesiology 122 (2015) 437–447, https://doi.org/10.1097/ALN.0000000000000558.
[24] T.K. Koo, M.Y. Li, A guideline of selecting and reporting intraclass correlation coefficients for reliability research, J. Chiropr. Med. 15 (2016) 155–163, https://doi.org/10.1016/j.jcm.2016.02.012.
[25] P. Schober, C. Boer, L.A. Schwarte, Correlation coefficients, Anesth. Analg. 126 (2018) 1763–1768, https://doi.org/10.1213/ANE.0000000000002864.
[26] E. Lanza, R. Muglia, I. Bolengo, O.G. Santonocito, C. Lisi, G. Angelotti, P. Morandini, V. Savevski, L.S. Politi, L. Balzarini, Quantitative Chest CT analysis in COVID-19 to predict the need for oxygenation support and intubation, Eur. Radiol. 30 (2020) 6770–6778, https://doi.org/10.1007/s00330-020-07013.2.
[27] E.R. DeLong, D.M. DeLong, D.L. Clarke-Pearson, Comparing the areas under two or more correlated receiver operating characteristic curves: a nonparametric approach, Biometrics 44 (1988) 837, https://doi.org/10.2307/2531595.
[28] S. McGee, Simplifying likelihood ratios, J. Gen. Intern. Med. 17 (2002) 647–650, https://doi.org/10.1046/j.1525-1497.2002.10750.x.
[29] A.W.E. Lieveld, B. Kok, F.H. Schuit, K. Azijli, J. Heijmans, A. Van Laarhoven, N. L. Assman, R.S. Kootte, T.J. Olgers, P.W.B. Nanayakkara, F.H. Bosch, Diagnosing COVID-19 pneumonia in a pandemic setting: Lung Ultrasound versus CT (LUVCT)-a multicentre, prospective, observational study, ERJ Open Res. 6 (2020) 00539–02020, https://doi.org/10.1183/23120541.00539-2020.
[30] S.L. Haak, I.J.E. Renken, L.C. Jager, H. Lameijer, B.B.Y.M. Van Der Kolk, Diagnostic accuracy of point-of-care lung ultrasound in COVID-19, Emerg. Med. J. 38 (2021) 94–99, https://doi.org/10.1136/emermed-2020-210125.
[31] D. Colombi, M. Petrini, G. Maffi, G.D. Villani, F.C. Bodini, N. Morelli, G. Milanese, M. Silva, N. Sverzellati, E. Michieletti, Comparison of admission chest computed tomography and lung ultrasound performance for diagnosis of COVID-19 pneumonia in populations with different disease prevalence, Eur. J. Radiol. 133 (2020), https://doi.org/10.1016/j.ejrad.2020.109344.
[32] X. Ding, J. Xu, J. Zhou, Q. Long, Chest CT findings of COVID-19 pneumonia by duration of symptoms, Eur. J. Radiol. 127 (2020), 109009, https://doi.org/10.1016/j.ejrad.2020.109009.

[33] F. Pan, T. Ye, P. Sun, S. Gui, B. Liang, L. Li, D. Zheng, J. Wang, R.L. Hesketh, L. Yang, C. Zheng, Time course of lung changes at chest CT during recovery from coronavirus disease 2019 (COVID-19), Radiology 295 (2020) 715–721, https://doi.org/10.1148/radiol.2020200370.

[34] B. Li, X. Li, Y. Wang, Y. Han, Y. Wang, C. Wang, G. Zhang, J. Jin, H. Jia, F. Fan, W. Ma, H. Liu, Y. Zhou, Diagnostic value and key features of computed tomography in Coronavirus Disease 2019, Emerg. Microbes Infect. 9 (2020) 787–793, https://doi.org/10.1080/22221751.2020.1750307.

[35] Y. Yang, Y. Huang, F. Gao, L. Yuan, Z. Wang, Lung ultrasonography versus chest CT in COVID-19 pneumonia: a two-centered retrospective comparison study from China, Intensive Care Med. 46 (2020) 1761–1763, https://doi.org/10.1007/s00134-020-06096-1.

[36] G. Soldati, A. Smargiassi, R. Inchingolo, D. Buonsenso, T. Perrone, D.F. Briganti, S. Perlini, E. Torri, A. Mariani, E.E. Mossolani, F. Tursi, F. Mento, L. Demi, On lung ultrasound patterns specificity in the management of COVID-19 patients, J. Ultrasound Med. 39 (2020) 2283–2284, https://doi.org/10.1002/jum.15326.

[37] M.M.G. Leeflang, P.M.M. Bossuyt, L. Irwig, Diagnostic test accuracy may vary with prevalence: implications for evidence-based diagnosis, J. Clin. Epidemiol. 62 (2009) 5–12, https://doi.org/10.1016/j.jclinepi.2008.04.007.

[38] W. Lu, S. Zhang, B. Chen, J. Chen, J. Xian, Y. Lin, H. Shan, Z.Z. Su, A clinical study of noninvasive assessment of lung lesions in patients with coronavirus disease-19 (COVID-19) by bedside ultrasound, Ultraschall Der Medizin – Eur. J. Ultrasound 41 (2020) 300–307, https://doi.org/10.1055/a-1154-8795.